Experimental and Modeling of Tetracycline degradation in water in a Flow-Through Enzymatic monolithic reactor

Sher Ahmad, Wassim Sebai, Marie-Pierre Belleville, Nicolas Brun, Anne Galarneau, José Sanchez-Marcano

▶ To cite this version:

HAL Id: hal-03705382

https://hal.umontpellier.fr/hal-03705382

Submitted on 27 Jun 2022

Experimental and Modeling of Tetracycline degradation in water in a Flow-Through Enzymatic monolithic reactor

Sher Ahmad[1], Wassim Sebai[1,2], Marie-Pierre Belleville[1], Nicolas Brun[2], Anne Galarneau[2], José Sanchez-Marcano[1*]

[1]Institut Européen des Membranes, Univ Montpellier, CNRS, ENSCM, Montpellier, France.

[2]Institut Charles Gerhardt Montpellier, Univ Montpellier, CNRS, ENSCM, Montpellier, France.

*Corresponding author:

Tel: +33 467149149; *Fax*: +33 467149119; *Email address*: Jose.Sanchez-Marcano@umontpellier.fr

Abstract

In this work, the laccase from *Trametes versicolor* was immobilized in highly porous silica monoliths (0.6 cm diameter, 0.5 cm length). These monoliths feature a unique homogeneous network of interconnected macropores (20 μm) with mesopores (20 nm) in the skeleton and a high specific surface area (330 m^2/g). The enzymatic monoliths were applied to degrade tetracycline (TC) in model aqueous solutions (20 ppm). For this purpose, a tubular Flow-Through-Reactor (FTR) configuration with recycling was built. The TC degradation was improved with oxygen saturation, presence of degradation products and recirculation rate. The TC depletion reachs 50% in the FTR and 90% in a stirred tank reactor (CSTR) using crushed monoliths. These results indicate the importance of maintaining a high co-substrate concentration near active sites. A model coupling mass transfers with a Michaelis-Menten kinetics was applied to simulate the TC degradation in real wastewaters at actual TC concentration (2.8 10^{-4} ppm). Simulation results show that industrial scale FTR reactor should be suitable to degrade 90% of TC in 5 h at a flow rate of 1 mL/min in a single passage flow configuration. Nevertheless, the process could certainly be further optimized in terms of laccase activity, oxygen supply near active sites and contact time.

1   Introduction

Pharmaceutical products (PPs) are found more and more frequently in the environment due to an increase in their consumption, because humains have a better access to medicines in conjunction with the aging of the population. Indeed, they can be found at very low concentrations ($\mu g\ L^{-1}$- $mg\ L^{-1}$) in wastewaters (Halling-Sørensen et al., 1998), rivers (Burns et al., 2018), sediments (Kerrigan et al., 2018) and sea (Björlenius et al., 2018). Moreover, traditional wastewater treatment plants (WWTP) are inefficient to completely remove PPs, (Alvarino et al., 2018; Thiebault et al., 2017; Verlicchi et al., 2012). Therefore, PPs remain in WWTP effluents and as a consequence they can be transferred to underground or surface waters, which are among the main sources of drinking water (Bruce et al., 2010; de Jongh et al., 2012). Several tertiary treatments have been proposed to improve the removal of PPs from wastewaters, they include advanced oxidation treatments (Kanakaraju et al., 2018; Kıdak and Doğan, 2018), physical adsorption (Rajapaksha et al., 2019 ; Rocha et al., 2020) or even enzymatic degradation.

Enzymatic degradation of PPs can be an alternative option among the other tertiary treatments named previously, since enzymes mediate biochemical reactions at a rapid rate under mild operating conditions (pH, temperature, solvents, and ionic strength). In particular, oxidoreductase enzymes such as laccases, tyrosinases and peroxidases have the ability to oxidize large variety of PPs like phenols, drugs, and hormones (Singh Arora and Kumar Sharma, 2010; Demarche et al., 2012; De Cazes et al., 2014). Nevertheless, enzymatic process can be expensive and unsustainable if enzymes are not recycled within the system.

Immobilization generally increases the stability of enzymes under reaction conditions while allowing their reuse and then reducing costs. (Zhang et al., 2015 Ji et al., 2017). Several immobilization techniques like adsorption, entrapment and encapsulation have been applied for enzyme immobilization on solid supports however it is observed that covalent immobilization enhances enzymes stability and long-term process sustainability (Zdarta et al., 2018). Along with nature of enzymes and immobilization techniques, choosing suitable solid support is also very essential in enzymatic process. Inorganic support materials like silica, zirconia, active carbons have high mechanical strength and temperature stability therefore are explored for immobilization of enzymes (Sadeghzadeh et al., 2020; Bebić et al., 2020; Zdarta et al., 2020).

The application of enzymatic reactors for PPs degradation has been explored with different configurations like packed bed reactors (Nguyen et al., 2016; Bilal and Iqbal, 2019), fluidized bed reactors (Lloret et al., 2012; Piao et al., 2019) as well as enzymatic membrane reactors (EMR) (de Cazes et al., 2014; Barrios-Estrada et al., 2018). EMRs have been widely studied for PPs degradation because they combine two functions in a single unit: filtration and enzymatic reaction (Sanchez Marcano and Tostsis, 2002; Sanchez Marcano, 2019). Nevertheless, EMRs can also present some drawbacks like membrane clogging or low reactivity because the amount of biocatalyst grafted on the separative layer of membranes is relatively low.

Ji et al., (2016) observed less than 10 % of carbamazepine degradation with laccase from *Trametes versicolor* in an EMR without using mediators. De Cazes et al., (2014) found only 56 % of tetracycline (TC) degradation in 24 h with laccase from *Trametes versicolor* immobilized on ceramic membranes. Similarly, Barrios-Estrada et al., (2018) found that only 33% of bisphenol-A was degraded in 24 h with an immobilized laccase on the same type of membranes. To overcome some of these disadvantages, meso-/macroporous monoliths have been recently applied for enzyme immobilization, the objective is to provide a big surface area to immobilize a large amount of enzymes, together with a macroporosity which allows low pressure drop while avoiding clogging (Ahmad et al., 2021; Biggelaar et al., 2019; Sebai et al., 2022). Moreover, as far as substrates are forced to flow through the monolith porosity the probability of contact with the biocatalyst is enhanced while allowing a precise control of the contact time (Sanchez Marcano, 2019). This configuration is called Flow-Trough-Reactor (FTR). Silica monoliths prepared by emulsion templating and presenting a large distribution of macropores (50 nm to 6 µm) have been recently used as supports in biocatalysis (Biggelaar et al., 2017, 2019). Another type of silica monoliths have been prepared by spinodal decomposition. They featured a narrow distribution of macropores and presented the advantage of an independent control of macropores (in the range 1 to 50 µm) and mesopores diameters (in the range 4 to 30 nm, with a corresponding to surface area of 800 to 200 $m^2\ g^{-1}$, respectively) (Fajula and Galarneau, 2019; Galarneau et al., 2016b, 2016a).

There are few reported models of mass transport through monoliths. They consider the macroscopic structure and developed approaches for simulation of velocity fields, diffusion, and dispersion of chemical species within the porous structure (Jungreuthmayer et al., 2015; Meyers and Liapis, 1999; Tallarek et al., 2002). These models, which are based on morphology and real structure of porous monoliths, require high computational techniques like image processing techniques as well as relatively large computing times and costs (Jungreuthmayer et al., 2015). This assertion is especially true for large-scale geometries required for practical engineering problems. Furthermore, apart from the recent work of Ahmad et al., (2021), no work has been reported in the literature coupling a reaction kinetics with transport of species within macroporous silica monoliths for scale-up purposes.

The objective of this research work was to develop an original FTR configuration using enzymatic monoliths for PPs degradation and studying by modeling and simulation the possibility of scale-up of the FTR for this application. For this purpose the degradation of tetracycline (TC) was chosen as model molecule of PPs. Firstly, a lab scale set up was used for stuying experimentally the enzymatic degradation of TC by laccase from *Trametes versicolor* covalently immobilized on silica monoliths with large homogeneous macropores (~20 µm) to assess low pressure drop and mesopores of 20 nm providing a large surface area (330 $m^2\ g^{-1}$) to improve enzymes immobilization. TC degradation tests were carried out in a tubular FTR configuration with recycling for the degradation of TC in aqueous solutions. Oxygen effect on TC degradation as well as the effect of TC degradation products on degradation rate were also studied. Morevoer, a previous reported

90 model (Ahmad et al., 2021) coupling mass transfers with an apparent Michaelis-Menten kinetics, determined

91 under oxygen saturation conditions, was applied to simulate the TC degradation in real wastewaters having

92 a TC concentration six orders of magnitude lower than oxygen concentration at saturation conditions at 25

93 °C. The developed model was employed to simulate the geometrical scale up of monoliths for the complete

94 TC degradation at usual real wastewater concentrations at different flows. To our knowledge, it is the first

95 time that such a study of TC degradation in a FTR has been carried out considering the influence of oxygen

96 as co-substrate and the degradation products and performing the scale-up for an actual concentration of this

97 antibiotic in wastewaters.

98

2 Materials and Methods

Silica monoliths with hierarchical porosity were synthesized and functionalized by amino groups for being used as solid support for covalent immobilization of laccases. The laccase-monoliths were then used for the removal of tetracycline (20 ppm) contained in water in batch and in flow through configuration. conditions using a recycling configuration. The effects of recirculation flow rate, of oxygen and presence of by-products were analyzed. Simulation was performed to evaluate the performance of laccase-monoliths for the removal of tetracycline in concentration (2.8×10^{-4} ppm) found in real wastewaters and to determine the size of monoliths necessary to treat efficiently such effluents in flow condition using a single passage configuration.

2.1 Materials

Powdered commercial laccase (activity ≥ 0.5 U mg^{-1} according to the provider), Tetracycline (TC) ($\geq 98.0\%$), Glutaraldehyde (GLU) (25% v/v) and 2,2'-azino-bis (3-ethylbenzothiazoline-6-sulphonic acid) (ABTS) were all purchased from Sigma-Aldrich, Germany.

Silica monoliths with macropores of 20 μm and mesopores of 20 nm diameters (specific surface area of 330 m^2 g^{-1}) were prepared by a controlled sol-gel process with tetraethylorthosilicate (TEOS) and polyethylene glycol (PEO) 100 kDa in acidic solution (HNO$_3$) followed by a basic treatment (NH$_4$OH 0.1 M) at 100 °C for 24 h and then calcined at 550 °C for 8 h, according to a method previously reported (Galarneau et al., 2016a). The monoliths were then activated at 250 °C under vacuum for 4 h to remove water prior to be grafted with 3-aminopropylamine triethoxysilane (APTES) in ethanol under reflux (80 °C) overnight with an excess of 10 amino groups per nm^2. The resulting NH$_2$-monoliths presented a grafting density of 1.5 NH$_2$/nm^2 corresponding to an amount of 0.8 mmol NH$_2$/g and leading to a specific surface area of 197 m^2 g^{-1}. The NH$_2$-monoliths were then cladded with a Teflon heat shrinkable gain at 180 °C for 2 h connected to stainless-steel tubing (Ahmad et al., 2021).

121 **2.2   Activation of monoliths and laboratory scale setup for TC degradation in water** Cladded NH$_2$-
122 silica monoliths were activated with a GLU solution (4% v/v) prepared in citrate phosphate buffer (pH 7, 0.1
123 M). Then, monoliths were filled with 0.5 mL of laccase solution (5±1 U mL^1) prepared by solubilizing the
124 necessary amount of commercial powder of enzyme in the same citrate phosphate buffer. After
125 immobilization, the resulting laccase-monoliths were stored in the buffer solution (pH 7) at 4 °C. The
126 measurement of the enzymatic activity of laccase immobilized in monoliths, was carried out through the
127 oxidation of 1 mM solution of 2,2-azino-bis(3-ethylbenzothiazoline-6 sulfonic acid (ABTS) at pH = 4. For
128 this purpose, the laccase-monoliths were crushed, and experiments were carried out in a stirred tank reactor
129 (25-50 mL) under vigorous magnetic agitation at 200 rpm. The same methodology was applied for the
130 determination of kinetic constants of TC degradation. Immobilization methods and activity determination of
131 crushed laccase-monoliths were described in detail in a previous publication (Ahmad et al., 2021).

132 A laboratory scale set up for TC degradation (Figure 1) was built by connecting in series three cladded
133 enzymatic monoliths (0.6 cm diameter, 0.5 cm length, ~50 mg, each). A HPLC pump (Gibson model: 321,
134 France) allowed recycling a TC solution in between the monoliths and a reservoir. A pressure transducer
135 (Keller, 0-2 bar) was connected before the inlet of the monoliths to monitor the pressure changes during the
136 process. The temperature of the feed tank was controlled placing the feed tank in a thermostatically controlled
137 water bath. All the TC degradation tests were carried out in closed loop (complete recycling of the TC
138 solution (20 ppm)) because of low TC degradation in a single pass. A TC solution (20 ppm, 30 mL) was
139 flowed through the monoliths at three different flow rates (0.5, 1 and 5 mL min^{-1}). In additional experiments,
140 air was bubbled in the feed tank solution at the air flow rate of 30-40 mL min^{-1} to keep feed TC solution at
141 oxygen saturation (measured with a DO meter VisiFerm RS-485 from Himlton (Switzerland)). Based on the
142 macropore volumes of the monolith (3.41 mL/g), we can estimate the number of times (cycles) the solution
143 passes through the FTR built with three enzymatic monoliths in series (~150 mg) (Table 1):

144

145 **Table 1.** Number of cycles through the laccase-monoliths reactor as a function of flow rate

Flow rate (mL/min)	Number of cycles in 24h (Vmacro: 3.41 mL/g)
0.5	1409
1	2818
5	14090

146

147 The Reynolds number (Re) (Bird, et al, 1960) was calculated from the well known following equation:

$$Re = \frac{\rho u d_{macro}}{\mu} \tag{1}$$

148

149 with ρ (0.997047 kg m^{-3}) the density of water at 25 °C, μ (0.000891 kg m^{-1} s^{-1}) the dynamic viscosity of water

150 at 25 °C, d_{macro} (2 10^{-5} m) the macropores mean diameter and u (m s^{-1}) the velocity of water within

151 macropores, u = V/A with V the flow rate (5 10^{-4} to 5 10^{-3} L min^{-1}) and A the section of the monolith (6 mm

152 diameter).

153 For comparison batch experiments were carried out with crushed laccase-monoliths (~150 mg) in a stirred

154 tank reactor (CSTR 50 mL) containing 30 mL of TC solution (20 ppm) under magnetic stirring (200 rpm).

155 In this case also additional experiments were carried out by bubbling air in the solution at the air flow rate of

156 30-40 mL min^{-1} to maintain oxygen saturation conditions. Samples of 100 μL were taken from feed tank

157 every 30 min to measure the TC concentration evolution during 24 h by HPLC-MS analysis (Waters 2695

158 separation module with micromass detector of Wythenshawe, Manchester, UK). Degradation products of TC

159 were separated and identified by means of liquid chromatography coupled to high resolution mass

160 spectrometer QExactive (LC-HRMS) equipped with a HESI ionization source operating in negative or

161 positive ionization mode, in separate injections. Data acquisition was performed in data dependent scan

162 where the 10 most intense ions from full scan (m/z 50-600) were further fragmented with an isolation of 1.0

163 Da at a collision energy of 30 a.u. Data results were processed manually with Xcalibur 3.1 software (IDAEA-

164 CSIC laboratory, Spain).

Control experiments to study the effect of TC self-degradation or adsorption on the evolution of TC concentration were carried out with whole or crushed inactivated enzymatic monoliths. For this purpose, enzymatic monoliths were deactivated by heating in oven at 100 °C for 2 h.
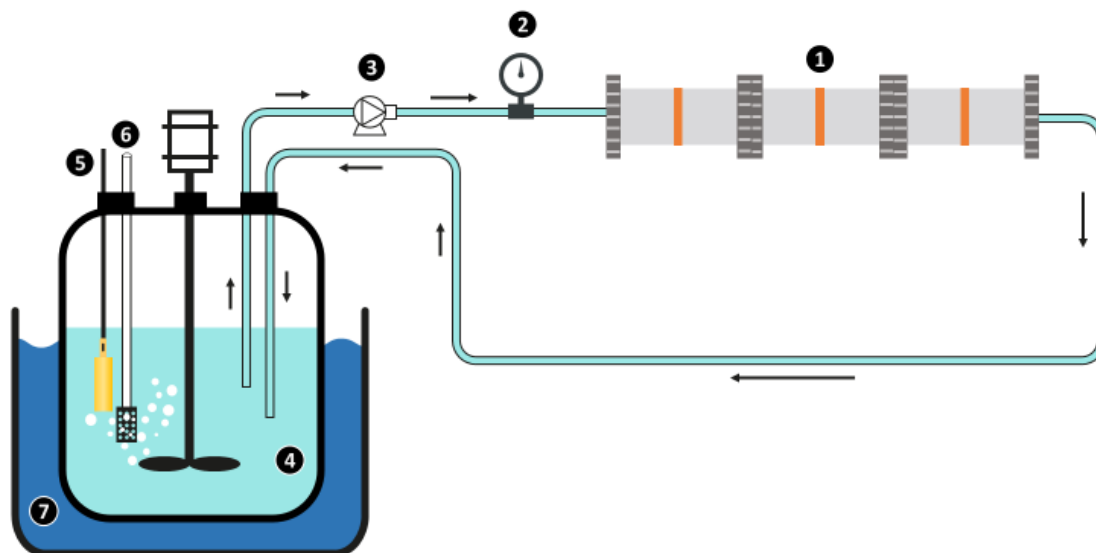
Figure 1. Schematic draw of the laboratory scale set up for TC degradation with recycling. 1: reactor composed of three monoliths in series, 2: pressure transducer, 3: HPLC pump, 4: Stirred tank with TC solution, 5: air bubbling system, 6: thermocouple, 7: Thermostatic water bath.

3   Results and discussions

3.1   Effect of recirculation rate on TC degradation

Recirculation rate in enzymatic reactor is an important parameter for continuous flow. When the recirculation rate is slow, the reaction can behave a similarly as non-continuous processes (Hamam and Budge, 2010) with a long contact time with the enzymes. When the recirculation rate is fast, more oxygen is is transported close to the enzymes, but the contact time is shorter. Therefore, it was important to determine the optimum flow rate for the TC degradation.

To study the effect of recirculation flow, TC degradation tests were carried out using the set up shown in Figure 1 at different recirculation flow rates from 0.5 to 5 mL min^{-1} at 25 °C. For each test, fresh laccase-monoliths were used with initial TC solution concentration of 20 ppm and total volume of TC solution of 30 mL. The decrease in relative TC concentration was similar for all flow-rates (Figure 2): 30% of the TC was degraded in the first five hours. For longer time reaction the degradation rate was extremely low (about 10% of additional degradation over the next 20 hours). This effect was observed with all tested recirculation flow

9

185 rates, which means that there was no effect of flow rate on the TC degradation. This indicates that the
186 transport of substrates inside the reactors containing the enzymes immobilized on silica monoliths is
187 governed by the self-diffusion in the mesopores and not by external mass transfer in the macropores.

188 The increase of the flow rate did not allow modifying the hydrodynamic flow regime. Indeed, the Reynolds
189 number (Re) calculated from Eq (1) for the recirculation flow rates of 0.5 to 5 mL min^{-1} was ranged between
190 0.01 - 0.1 and corresponded for all flow rates to a laminar flow regime (limit of the laminar flow regime (Re
191 < 1) (Bird et al, 1960). It can be concluded that the increase in flow rate was not high enough to further
192 decrease possible external mass transfer resistances (decrease of boundary layers). In previous studies,
193 Galarneau et al., (2016b) studied the dependence of flow rate on external mass transfer layer with silica
194 monoliths for Diels-Alder reaction. They observed that productivity was increased by increasing the flow
195 rate from 0.01 to 0.03 mL min^{-1}. In another study, Jatoi et al., (2021) studied the effect of flow rate on
196 external mass transfer limitations with silica monoliths loaded with Pt in the continuous-flow liquid-phase
197 hydrogenation of *p*-Nitrophenol. They observed that for the range of flow rate from 1 to 8 mL min^{-1} there
198 was no effect on mass transfer limitations in macropores and attributed this behavior to the relative "high"
199 flow rate applied. From these results it can be concluded that boundary layer reduction and optimium flow
200 depends on several other factors like reaction rate, substrate concentration, pore size and porosity, which
201 needs to be optimized as well.

202

203
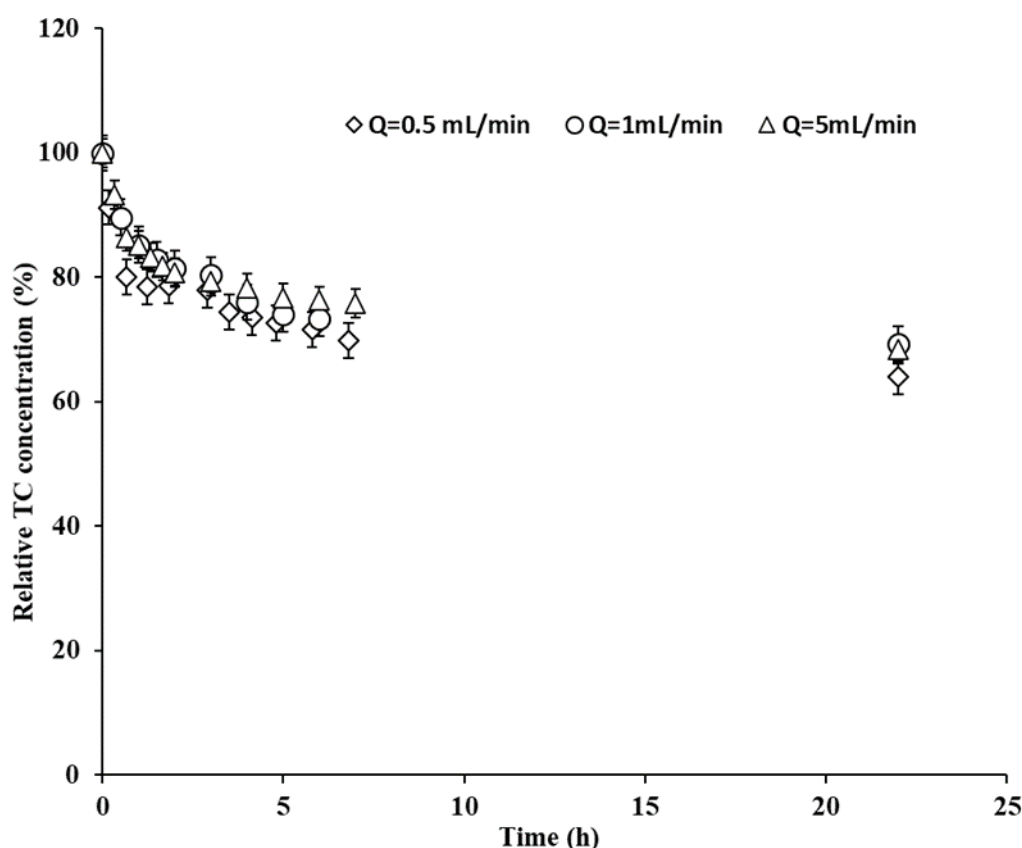
Figure 2. TC degradation at different flow rates (0.5-5 mL min^{-1}). Temperature: 25°C; TC initial concentration of 20 ppm; total volume of TC solution of 30 mL, 15 U of enzymes in laccase-monoliths.

206

There are other possible explanations to the low experimental TC degradation (Figure 2). For example, the process can be controlled by internal mass transfer, i. e. diffusion inside the mesopores, which can be considered as stagnant regions in monoliths. In fact, silica monoliths feature skeletons with a thickness in the range 5-15 μm, which contain an interconnected mesoporous structure where the major part of enzyme molecules is immobilized. Therefore, the most part of reactive sites inside the mesoporous structure are only accessible through the diffusion of substrates.

213

3.2   Effect of dissolved oxygen on TC degradation

Laccases, are multicopper oxidases that catalyze the oxidation of different aromatic compounds with molecular oxygen, which is concomitantly reduced to water (Nyanhongo et al., 2012). In order to study the importance of the amount of oxygen available for ~~on~~ TC degradation, the effect of the addition of air bubbling at a flow rate of 30-40 mL min^{-1} was first studied in a stirred tank reactor with crushed monoliths as discussed

219　in section 2.2 (Figure 3). The concentration of the dissolved oxygen in the tank was measured during the

220　experiments with and without air-bubbling (Figure 4).

221
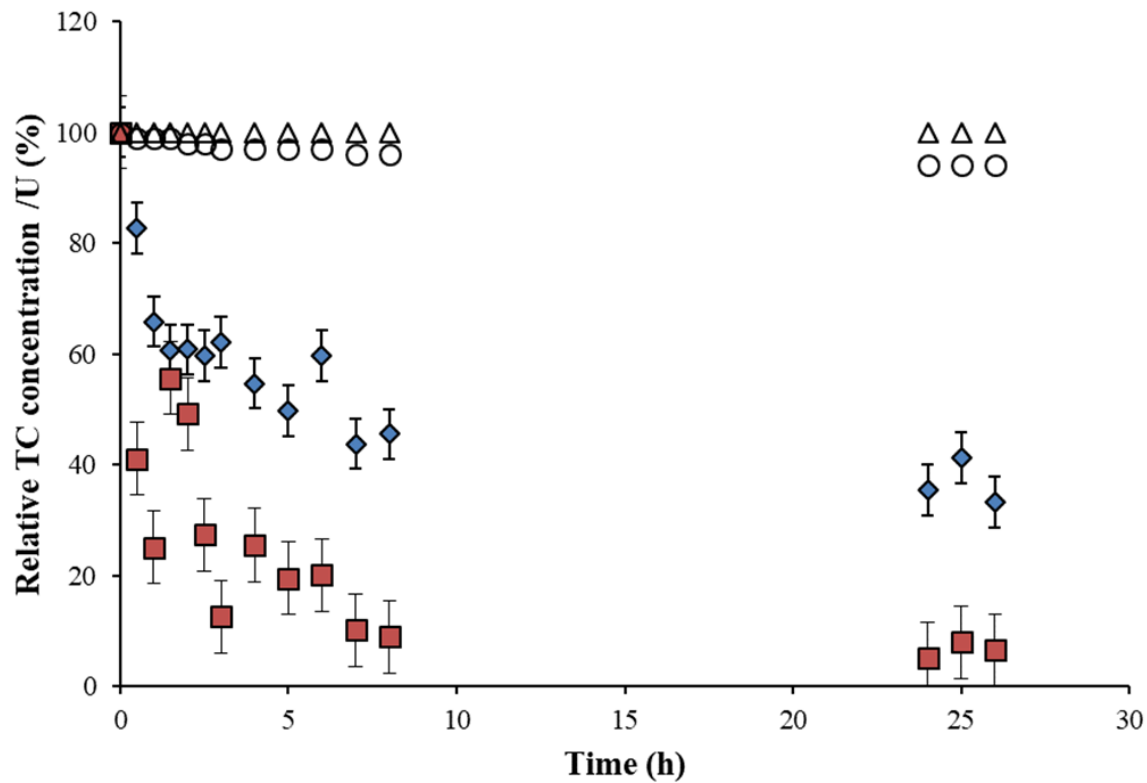
Figure 3. Evolution of TC concentration with crushed laccase-monoliths in a stirred tank reactor, without
(diamonds) and with (squares) air-bubbling. Control experiments with inactivated laccase-monoliths with
(circles) and without (triangles) air bubbling. Initial TC concentration of 20 ppm in osmosed water (pH 6).
Enzyme concentration of 18 U in the laccase-monoliths. Total volume 30 mL, temperature 25 °C.
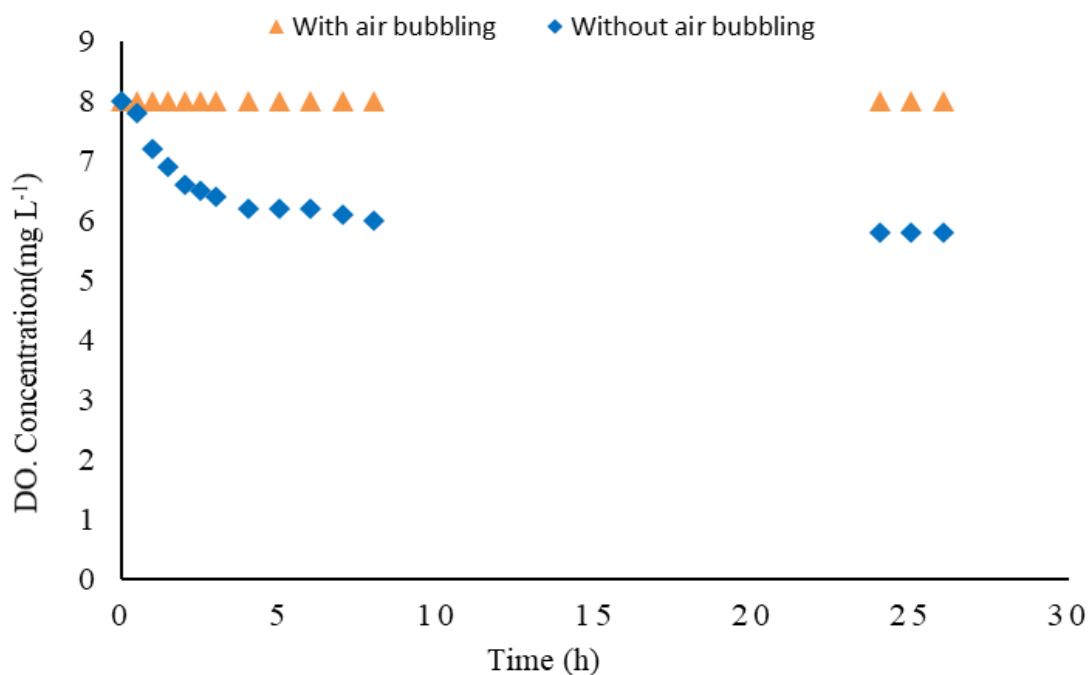
Figure 4. Evolution of dissolved oxygen (DO) concentration verse time in case of TC degradation test with crushed laccase-monoliths in a stirred tank reactor with (triangles) or without (diamonds) air bubbling. Initial TC concentration of 20 ppm in osmosed water (pH 6). Enzyme concentration of 18 U in the laccase-monoliths. Total volume 30 mL, temperature 25 °C.

From Figure 3 it can be observed that for control tests (with inactivated laccase-monoliths) TC self-degradation or adsorption (with or without air bubbling) was extremely low (less than 5%). ~~Furthermore,~~ For the crushed active monoliths without air bubbling the TC degradation was 55% in the first 6 h, while with air bubbling, the TC degradation reached more than 90% in the same period. These results show that oxygen seems to be a limiting substrate for TC degradation. The same conclusion was found in literature (Ortner et al., 2015) for the oxidation of lignins using laccase from *Trametes villosa*. The authors observed a rapid decrease of oxygen concentration at the beginning of the reaction, which limited the oxidation of phenolic compounds. They concluded that a sufficient oxygen concentration is necessary for an efficient laccase oxidation process. In the present work, when the solution was bubbled with air, the dissolved oxygen (DO) was always at saturation value (~8.3 mg L^{-1} at 25 °C) (Figure 4), which corresponded to an excess of 5.6 moles of oxygen/moles of TC. Without air bubbling, the DO concentration decreased of 20% in the first 6 h concomitantly with the decrease of TC concentration (55%) to reach a steady-state of DO concentration of 6 mg L^{-1}. The calculation of the number of moles of TC and oxygen (5.6 10^{-6} and 1.35 10^{-6}, respectively) indicates that a final molar ratio O_2/TC of 4, is therefore not enough to proceed to further oxidation. An excess of at least 5.6 O_2 molecules per TC seems to be necessary for total TC oxidation.

247 The effect of air bubbling in the FTR was studied at two different flow rates (1 and 5 mL min^{-1}) by bubbling

248 air inside the feed tank (30-40 mL min^{-1}) (Figure 5). Initial TC concentration for each experiment was 20

249 ppm, the total volume of solution in the tank was 30 mL and the total activity of the 3 cladded laccase-

250 monoliths was 12 U. For the flow rate of 5 mL min^{-1}, the degradation of TC reached 50 % with air bubbling,

251 while without air bubbling the TC degradation was only 30%. Similarly, for the flow rate of 1 mL min^{-1}, the

252 TC degradation was 40 and 30% with and without air bubbling, respectively. With air bubbling, TC

253 degradation was slightly higher in the case of the larger flow rate (5 mL min^{-1}) due to the larger amount of

254 oxygen provided to the reactor. Nevertheless, this TC degradation ratio remains low compared to 90% TC

255 degradation reached in a stirred tank reactor with air bubbling (Figure 5).
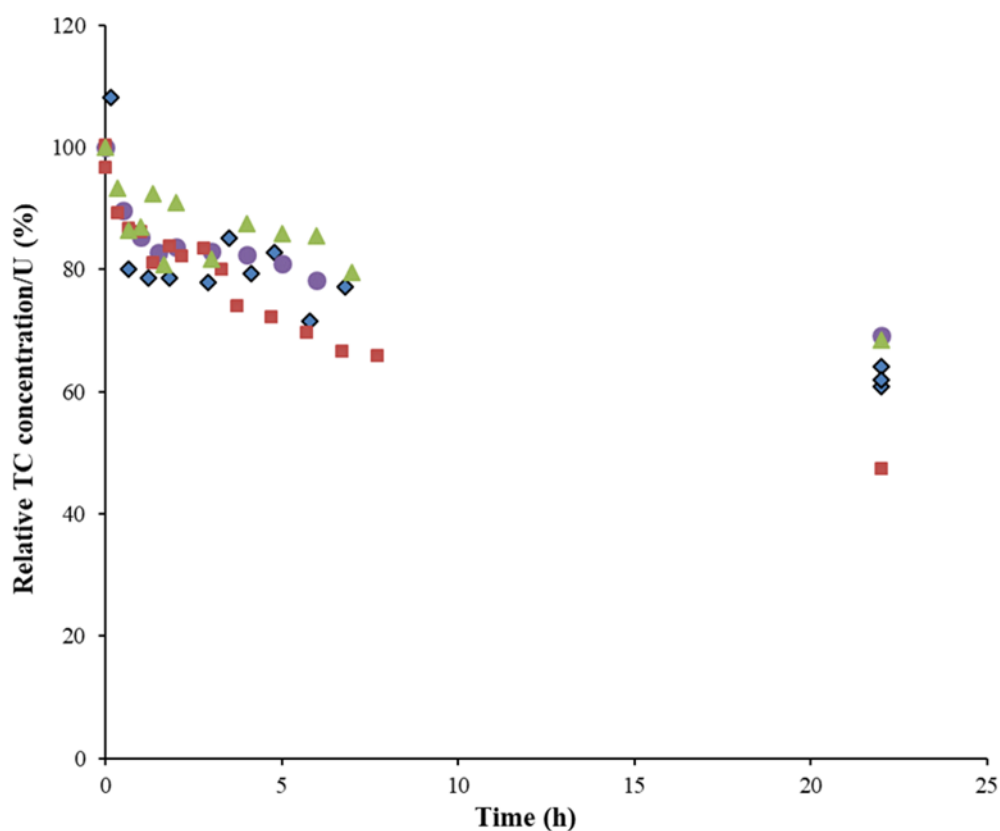
256

257 **Figure 5.** Evolution of TC concentration with laccase-monoliths under recycling flow at different flow rates

258 without air bubbling (TC solution flow rates: circle, 1 mL min^{-1}; triangle, 5 mL min^{-1}) and with air bubbling

259 (TC solution flow rates: diamonds, 1 mL min^{-1}; squares, 5 mL min^{-1}) at 25°C. Conditions: initial TC

260 concentration of 20 ppm in osmosed water; total volume of TC solution of 30 mL; total activity of the laccase-

261 monoliths of 12 U.

262

263 These results suggest the decrease of oxygen concentration near the bio-catalytic sites (which are located

264 everywhere in the surface of monoliths, but mainly inside the mesoporosity), which limits the reaction rate

14

265 and the conversion in flow. Furthermore, maintaining a high oxygen concentration or even an excess of
266 oxygen in the solution of the reservoir is not enough to enhance the conversion; this emphasizes that the
267 decrease of co-substrate (O_2) concentration near catalytic sites certainly controls the process.

268

3.3 Effects of TC degradation products

270 Many different TC degradation products were identified using the same laccase immobilized in ceramic
271 membranes (De Cazes., et al., 2014). These products present a TC based structure like anhydrotetracycline,
272 4-epi-anhydrotetracycline, dehydrooxotetracycline and 12-dehydrotetracycline (Llorca et al., 2015). In this
273 study the main molecules identified by LC-HRMS (IDAEA-CSIC laboratory, Spain) during the degradation
274 of TC are presented in Figure 6. One of the major products identified was dehydrooxytetracycline (m/z =
275 459.1396) obtained after hydroxylation of the tetracycline. Some other products were identified coming from
276 the loss of functional groups (-OH, -NH_2, etc.) of the tetracycline molecule. However the gap in the mass
277 balance between initial tetracycline and the amount of identified by-products indicates that the majority of
278 tetracycline was polymerized (as is usually the case for phenolic compounds), or completely oxydized into
279 CO_2 or transformed in other by-products, which were not detectable by LC-HRMS.

280
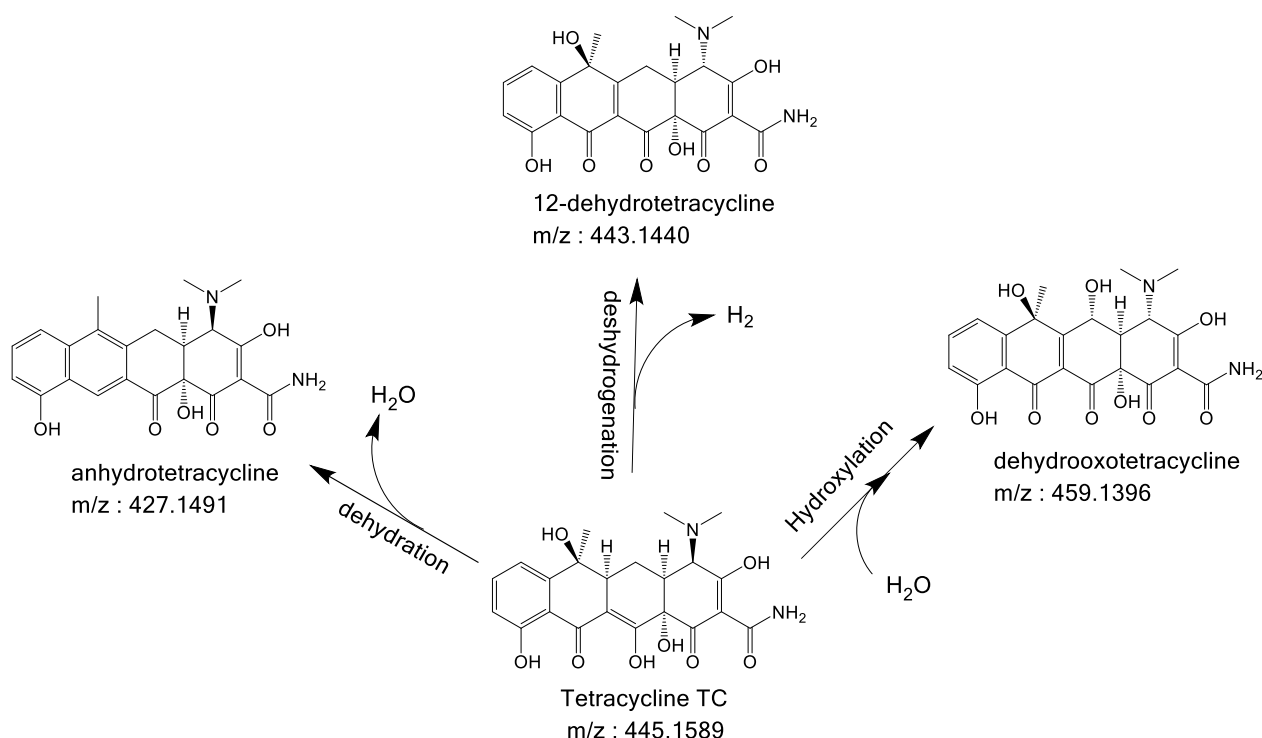
281

282 **Figure 6.** Degradation products of tetracycline and possible reaction pathways using laccase from *Trametes*
283 *versicolor* immobilized on silica monolith.

284

As enzymes can be inhibited by the products of the enzymatic conversion (Jing et al., 2009; Barth et al., 2015), the effect of degradation products on TC degradation rate was studied with crushed monoliths and under vigorous stirring to avoid any influence of mass transport limitations. For this purpose, an initial TC degradation test was carried out for 24 h, with 50 mL of fresh TC solution (20 ppm) and a total enzymatic activity of crushed monoliths of 6 U. After 24 h of reaction (without air bubbling), the reaction mixture (unconverted TC + degradation products) was separated from the immobilized enzymes by filtration. Afterward, a series of TC degradation experiments were carried out at different concentrations of degradation products by adding a volumetric fraction (50-90%) of the reaction mixture obtained from the initial experiment to a fresh TC solution (up to reach an initial TC concentration of 20 ppm) mixed with a fresh crushed enzymatic monolith (6 U). The results obtained are shown in Figure 7. It is important to notice that a lower degree of TC degradation (20%) was observed in comparison to the results (60% degradation) reported in Figure 3. This is due to the use of a lower enzymatic monolith activity (6 U instead of 18 U) .
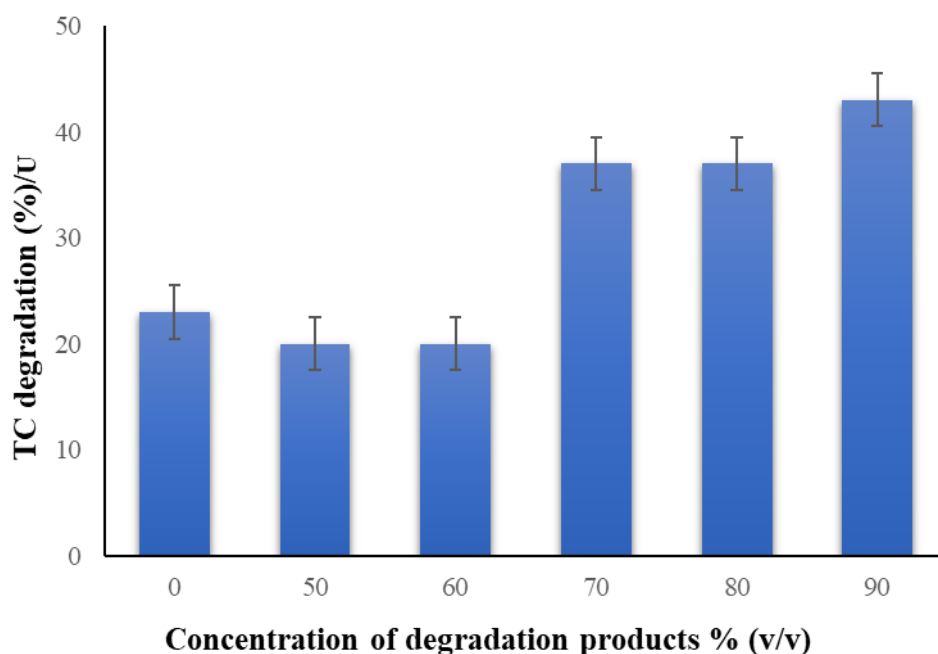
Figure 7. Effect of the amount of TC degradation products on TC degradation in batch. Initial TC concentration of 20 ppm; crushed laccase-monolith (6 U); temperature 25 °C; reaction time of 24 h.

The main result of this series of experiments is the enhancement of TC degradation with the increase of concentration of degradation products. Without degradation products and until a concentration of 60% of degradation products, TC degradation is around 20% in 24 hours, whereas for more than 70% of degradation products present in the solution, TC degradation reaches 40% after 24 hours. These results show that the TC degradation products formed did not inhibit the TC degradation, but in opposite they enhanced the conversion

16

when their concentration reached a minimum level. A similar phenomenon has been recently observed by Parra Guardado et al., (2019) and has been explained by the fact that some products of the reaction can act as redox mediators enhancing the enzyme reactivity and the conversion. This could also explain the higher degradation rate of TC (by a factor 2) obtained in the stirred tank reactor in comparison to the FTR, where degradation products do not spend enough time in the enzyme vicinity.

3.4 Application of a model for simulation of TC degradation in actual wastewater concentrations and proposed scale up of monolith system

In a previous work (Ahmad et al., 2021) reported a computational fluid dynamics (CFD) model allowing computing TC degradation. The model was built coupling an apparent Michaelis-Menten reaction kinetics of immobilized enzymes, flow hydrodynamics within the FTR and a dynamic mass balance on feed tank. As far as this model was built in conditions of oxygen saturation conditions and with a reaction kinetics, which only takes into account TC and not oxygen, it should not be applied for TC concentrations as high as used in this work (20 ppm). Indeed it was demonstrated here that oxygen becomes rapidly a limiting substrate. However, in some municipal wastewaters the TC concentration currently encountered is very low (2.8 10^{-4} ppm) (Abejón et al., 2015b; Danner et al., 2019). Thus, in this case and considering the saturation concentration of oxygen at 25 °C (8 mg L^{-1}), the concentration of O_2 ($O_2/TC = 4\ 10^5$) would be five orders of magnitude larger than the requirement previously founded ($O_2/TC = 5.6$). Under such conditions, we can consider that oxygen is no longer a limiting substrate and then the model can be reasonably applied for simulation purposes.
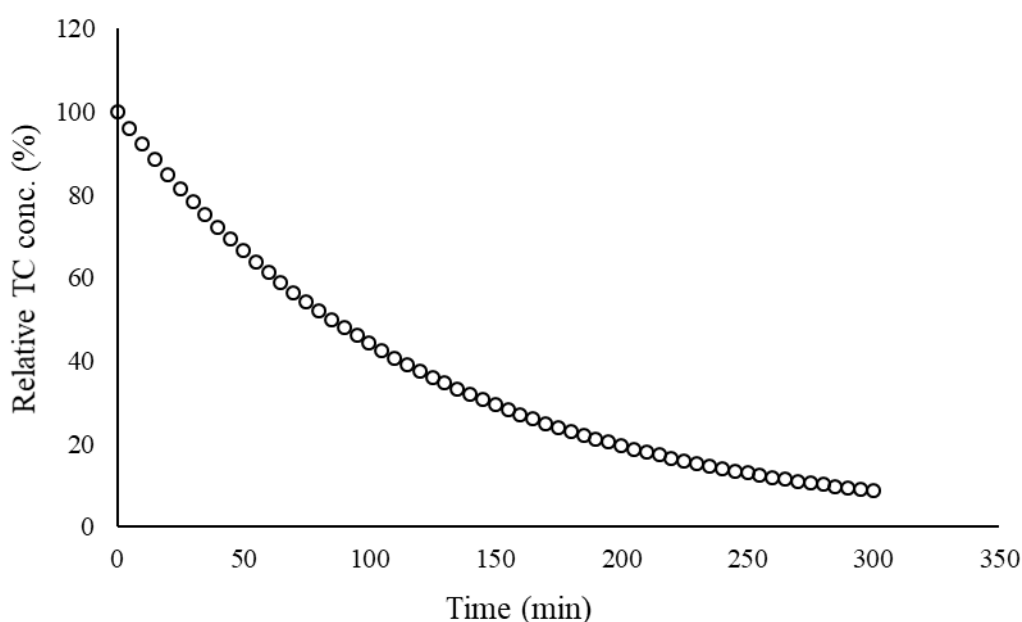
329 **Figure 8.** Simulated degradation of TC at actual initial TC concentration (2.8 10^{-4} ppm) found in wastewater

330 in a FTR. Simulation conditions: flow rate (1 mL min^{-1}), continuous recycled mode, Temperature 25 °C, 15

331 U of enzymatic activity in the monoliths.

332

333 The simulation of the TC degradation carried out with the FTR (3 monoliths in series of 0.6 cm diameter and

334 0.5 cm length, each) shows that for real TC concentration (2.8 10^{-4} ppm) a removal of 90% of TC was reached

335 in 5 h at a flow rate of 1 mL min^{-1} with a recycling configuration (see Figure 8). Taking account of these

336 results, we then proposed to determine the minimum size of a monolith that allows a complete degradation

337 of the TC in only one passage (without recycling) through the FTR. For this purpose, monoliths with different

338 size (length and diameter ranged in between 5-50 cm and 1-20 cm, respectively) were considered for

339 simulations (Table 2). When the size of monoliths is increased the conversion is enhanced. For example, for

340 a single pass, when the monolith geometry was set at 5 cm length and 1 cm diameter only 0.5% of initial TC

341 was converted. However, with monoliths of 50 cm length and 20 cm diameter it was possible to completely

342 degrade TC at a flow rate of 1 mL min^{-1}. These theoretical "large-scale monoliths" were then used for further

343 simulations.

344

345 **Table 2.** Effect of the scale up of the silica monoliths (by increasing the length and diameter of the monoliths)

346 towards TC degradation.

Length (cm)	Diameter (cm)	Inlet concentration (ppm) x10^{-4}	TC	Outlet concentration (ppm) x10^{-4}	TC	TC conversion in a single pass (%)
0.15	0.06	2.8		2.79		0.3
5	2	2.8		2.78		0.7
10	4	2.8		2.68		4
15	6	2.8		2.43		13
20	8	2.8		2.01		28
25	10	2.8		1.34		52
50	**20**	2.8		0		**100**

347

348 The TC conversion along the length of the optimum reactor (20 cm diameter, 50 cm length) was then studied

349 at different flow rates (Figure 9). Complete TC degradation was achieved at the flow rate of 1 mL min^{-1}.

18

350 However, it can be observed that the rate of TC depletion in the last 15 cm was relatively low; this last section

351 of the monolith is not enough efficient. For flow rates higher than 1 mL min^{-1}, TC conversion decreases up

352 to 50% at a flow rate of 5 mL min^{-1} (Figure 9). In fact, the global process is controlled by reaction kinetics

353 and at high flow rates, the residence time is too low to reach a complete TC depletion. However, as real

354 wastewater fluxes are extremely high (600-70,000 m^3/day) a compromise must be found between the level

355 of TC depletion, the contact time and process effectiveness. For this, an optimization has to be carried out

356 with multi-objective programming like Pareto optimality, this analysis has to be coupled with the cost of the

357 process (Abejón et al., 2015b).

358
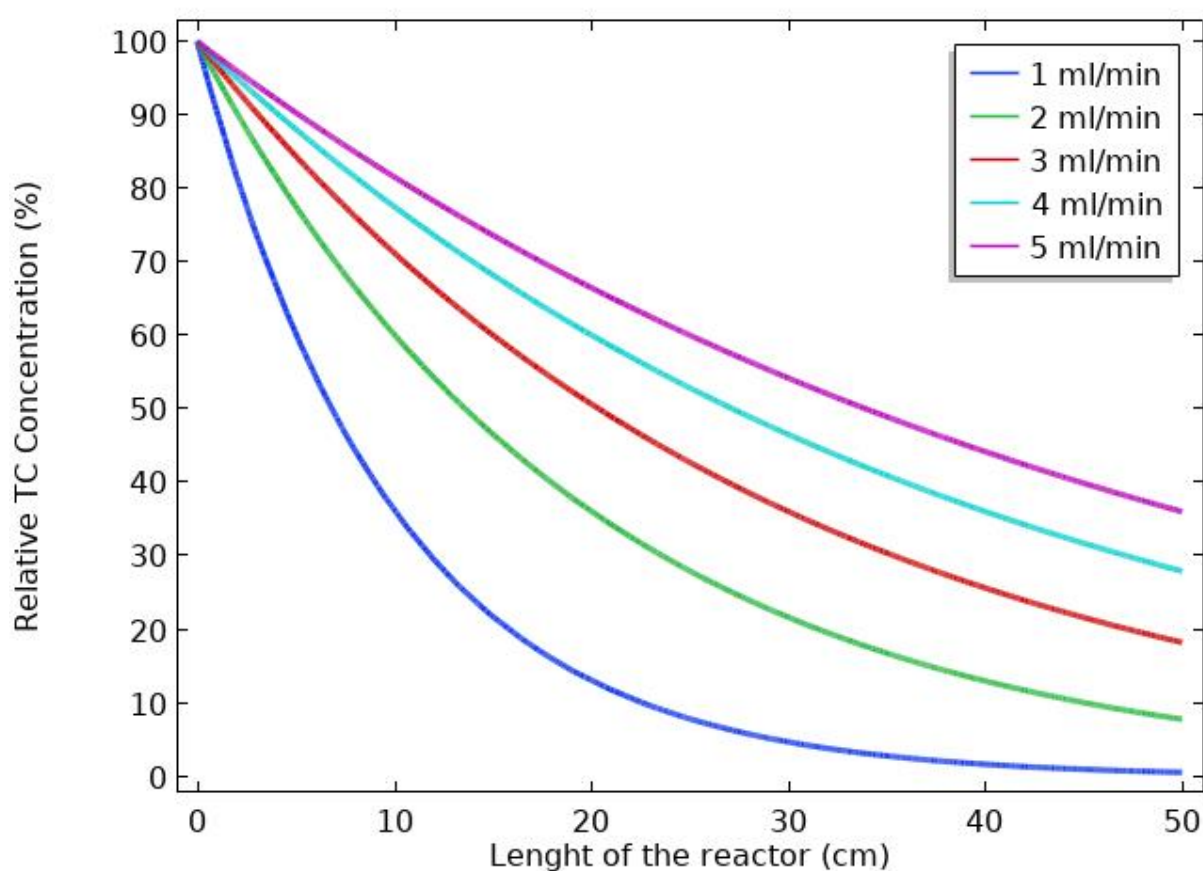
359

360 **Figure 9.** Relative tetracycline concentration along the length of the reactor from inlet to outlet at different

361 TC flow rates from 1 to 5 mL min^{-1}. Reactor length: 50 cm, diameter: 20 cm; Inlet TC concentration: 2.8 10^{-4}

362 ^{4} ppm; Reaction rate: 4.4 10^{-5} μmol L^{-1} min^{-1}.

363

364 **Conclusions**

365 Biocatalytic reactors were built by grafting laccase into the mesopores of macroporous silica monoliths. The

366 depletion of tetracycline (TC) (20 ppm) in aqueous solutions was carried out in a tubular flow through reactor

19

367 (FTR) configuration (3 monoliths in series of 0.6 cm diameter and 0.5 cm length, each) with recycling in a
368 reservoir tank. Only 30-40% of TC was degraded during the first 5 h and then the conversion slowed down
369 to a threshold. The increase of flow rate from 0.5 to 5 mL min^{-1} did not change TC depletion showing that
370 the phenomenon was not due to external mass transfer limitation, but rather to diffusion limitation of
371 substrates inside the mesopores. Experiments performed in stirred tank reactors (CSTR) with crushed
372 monoliths showed a higher TC depletion of 55% in 6 h, which was increased to 90% when the solution was
373 bubbled with air. This showed that O_2 is a limiting substrate for this reaction and that a molar excess of at
374 least 5.6 O_2/TC is necessary for a complete TC depletion. In FTR configuration, the addition of air-bubbling
375 in the reservoir lead to an increase of TC depletion of only 10%, with a maximum of 50% at flow rate of 5
376 mL min^{-1}, this result indicates that oxygen limitations are enhanced in FTR configuration due to the mass
377 transport limitations inside the mesopores. It was observed that the presence of by-products of degradation
378 increases the TC depletion, this result could be explained by a possible the role of redox mediators of such
379 by-products. In real municipal wastewater TC concentration is very low (2.8 10^{-4} ppm) and O_2 will be no
380 more a limiting substrate as its excess of 5 orders of magnitude higher than TC. The modeling of FTR showed
381 that in such conditions TC depletion should reach 90% in 5 h at a flow rate of 1 mL min^{-1} in a recirculating
382 flow mode. The model allowed to predict that a monolith of 20 cm diameter and 50 cm length could be used
383 for a total depletion of TC in a single pass (without recirculation) at a flow rate of 1 mL/min. However for
384 higher flow rates (as the one encountered in real wastewater treatments) the decrease of the TC depletion was
385 noticed. This is due by the fact that the depletion is governed by the reaction kinetic of the laccase. Further
386 improvement on laccase activity could contribute to optimize the process. New monolithic configurations
387 and processes have to be designed in order to feed oxygen continuously inside the porosity.

388

389 **Declarations**

390

391 **Ethics approval and consent to participate**

392 Not applicable

393

394 **Consent for publication**

395 Not applicable

396

Availability of data and materials

The datasets used and/or analyzed during the current study are available from the corresponding author on reasonable request, additional information and results are given in supplementary material.

Competing interests

The authors declare that they have no competing interests

Authors' contributions

Sher Ahmad and Wassim Sebai carried out the experimental work, synthesis of monoliths and enzymatic degradation of tetracycline, Marie-Pierre Belleville designed degradation experiments and contributed to the scientific discussion, Nicolas Brun, designed monoliths synthesis and contributed to the scientific discussion, Anne Galarneau and Jose Sanchez Marcano supervised all of the work, contributed with the discussions and wrote the whole manuscript. All of the authors revised the manuscript.

References

Abejón, R., Belleville, M.P., Sanchez-Marcano, J., 2015a. Design, economic evaluation and optimization of enzymatic membrane reactors for antibiotics degradation in wastewaters. Sep. Purif. Technol. 156, 183–199. https://doi.org/10.1016/j.seppur.2015.09.072

Abejón, R., De Cazes, M., Belleville, M.P., Sanchez-Marcano, J., 2015b. Large-scale enzymatic membrane reactors for tetracycline degradation in WWTP effluents. Water Res. 73, 118–131. https://doi.org/10.1016/j.watres.2015.01.012

Ahmad, S., Sebai, W., Belleville, M.-P., Brun, N., Galarneau, A., Sanchez-Marcano, J., 2021. Enzymatic monolithic reactors for micropollutants degradation. Catal. Today, 1st International Conference on Unconventional Catalysis, Reactors and Applications: Catalysis Beyond the Reactor 362, 62–71. https://doi.org/10.1016/j.cattod.2020.04.048

Almomani, F.A., Shawaqfah, M., Bhosale, R.R., Kumar, A., 2016. Removal of emerging pharmaceuticals from wastewater by ozone-based advanced oxidation processes. Environ. Prog. Sustain. Energy 35, 982–995. https://doi.org/10.1002/ep.12306

Alvarino, T., Lema, J., Omil, F., Suárez, S., 2018. Trends in organic micropollutants removal in secondary treatment of sewage. Rev. Environ. Sci. Biotechnol. 17, 447–469. https://doi.org/10.1007/s11157-018-9472-3

Barrios-Estrada, C., Rostro-Alanis, M. de J., Parra, A.L., Belleville, M.-P., Sanchez-Marcano, J., Iqbal, H.M.N., Parra-Saldívar, R., 2018. Potentialities of active membranes with immobilized laccase for Bisphenol A degradation. Int. J. Biol. Macromol. 108, 837–844. https://doi.org/10.1016/j.ijbiomac.2017.10.177

Barth, M., Oeser, T., Wei, R., Then, J., Schmidt, J., Zimmermann, W., 2015. Effect of hydrolysis products on the enzymatic degradation of polyethylene terephthalate nanoparticles by a polyester hydrolase from Thermobifida fusca. Biochem. Eng. J. 93, 222–228. https://doi.org/10.1016/j.bej.2014.10.012

Bebić, J., Banjanac, K., Ćorović, M., Milivojević, A., Simović, M., Marinković, A., Bezbradica, D., 2020. Immobilization of laccase from Myceliophthora thermophila on functionalized silica nanoparticles: Optimization and application in lindane degradation. Chin. J. Chem. Eng. 28, 1136–1144. https://doi.org/10.1016/j.cjche.2019.12.025

Biggelaar, L. van den, Soumillion, P., Debecker, D., 2019. Continuous Flow Mode Biocatalytic Transamination Using Macrocellular Silica Monoliths: Optimizing Support Functionalisation and Enzyme Grafting. https://doi.org/10.26434/chemrxiv.7853552.v1

Bilal, M., Iqbal, H.M.N., 2019. Lignin peroxidase immobilization on Ca-alginate beads and its dye degradation performance in a packed bed reactor system. Biocatal. Agric. Biotechnol. 20, 101205. https://doi.org/10.1016/j.bcab.2019.101205

Bird, R.B., Stewart, W.E., Lightfoot, E.N., 1960. Transport phenomena. New York: Wiley.

Björlenius, B., Ripszám, M., Haglund, P., Lindberg, R.H., Tysklind, M., Fick, J., 2018. Pharmaceutical residues are widespread in Baltic Sea coastal and offshore waters – Screening for pharmaceuticals and modelling of environmental concentrations of carbamazepine. Sci. Total Environ. 633, 1496–1509. https://doi.org/10.1016/j.scitotenv.2018.03.276

461 Burns, E.E., Carter, L.J., Kolpin, D.W., Thomas-Oates, J., Boxall, A.B.A., 2018. Temporal and spatial
462 variation in pharmaceutical concentrations in an urban river system. Water Res. 137, 72–85.
463 https://doi.org/10.1016/j.watres.2018.02.066

464 Cabana, H., Alexandre, C., Agathos, S.N., Jones, J.P., 2009. Immobilization of laccase from the white rot
465 fungus Coriolopsis polyzona and use of the immobilized biocatalyst for the continuous elimination of
466 endocrine disrupting chemicals. Bioresour. Technol. 100, 3447–3458. https://doi.org/10.1007/s10103-
467 009-0744-6

468 Danner, M.-C., Robertson, A., Behrends, V., Reiss, J., 2019. Antibiotic pollution in surface fresh waters:
469 Occurrence and effects. Sci. Total Environ. 664, 793–804.
470 https://doi.org/10.1016/j.scitotenv.2019.01.406

471 de Cazes, M., Belleville, M.-P., Petit, E., Llorca, M., Rodríguez-Mozaz, S., de Gunzburg, J., Barceló, D.,
472 Sanchez-Marcano, J., 2014. Design and optimization of an enzymatic membrane reactor for
473 tetracycline degradation. Catal. Today, Proceedings of the 11th International Conference on Catalysis
474 in Membrane Reactors 236, 146–152. https://doi.org/10.1016/j.cattod.2014.02.051

475 Demarche, P., Junghanns, C., Nair, R.R., Agathos, S.N., 2012. Harnessing the power of enzymes for
476 environmental stewardship. Biotechnol. Adv. 30, 933–953.
477 https://doi.org/10.1016/j.biotechadv.2011.05.013

478 François Fajula, Anne Galarneau, 2019. Combining Phase Separation with Pseudomorphic
479 Transformation for the Control of the Pore Architecture of Functional Materials: A Review. Pet. Chem.
480 59, 761–769. https://doi.org/10.1134/S0965544119080061

481 Galarneau, A., Abid, Z., Said, B., Didi, Y., Szymanska, K., Jarzębski, A., Tancret, F., Hamaizi, H.,
482 Bengueddach, A., Di Renzo, F., Fajula, F., 2016a. Synthesis and Textural Characterization of
483 Mesoporous and Meso-/Macroporous Silica Monoliths Obtained by Spinodal Decomposition.
484 Inorganics 4, 9. https://doi.org/10.3390/inorganics4020009

485 Galarneau, A., Sachse, A., Said, B., Pelisson, C.-H., Boscaro, P., Brun, N., Courtheoux, L., Olivi-Tran, N.,
486 Coasne, B., Fajula, F., 2016b. Hierarchical porous silica monoliths: A novel class of microreactors for
487 process intensification in catalysis and adsorption. Comptes Rendus Chim., Emerging Chemistry in
488 France 19, 231–247. https://doi.org/10.1016/j.crci.2015.05.017

489 Goi, A., 2005. Advanced oxidation processes for water purification and soil remediation, Thesis on
490 chemistry and chemical engineering. TTU Press, Tallinn.

491 Halling-Sørensen, B., Nors Nielsen, S., Lanzky, P.F., Ingerslev, F., Holten Lützhøft, H.C., Jørgensen, S.E.,
492 1998. Occurrence, fate and effects of pharmaceutical substances in the environment- A review.
493 Chemosphere 36, 357–393. https://doi.org/10.1016/S0045-6535(97)00354-8

494 Hamam, F., Budge, S.M., 2010. Structured and specialty lipids in continuous packed column reactors:
495 comparison of production using one and two enzyme beds. Journal of the American Oil Chemists'
496 Society 87, 385-394.

497 Iyer, P.V., Ananthanarayan, L., 2008. Enzyme stability and stabilization—Aqueous and non-aqueous
498 environment. Process Biochem., Metabolic Engineering 43, 1019–1032.
499 https://doi.org/10.1016/j.procbio.2008.06.004

500   Jatoi, H.U.K., Goepel, M., Poppitz, D., Kohns, R., Enke, D., Hartmann, M., Gläser, R., 2021. Mass
501   Transfer in Hierarchical Silica Monoliths Loaded With Pt in the Continuous-Flow Liquid-Phase
502   Hydrogenation of p-Nitrophenol. Front. Chem. Eng. 3.

503   Ji, C., Hou, J., Wang, K., Zhang, Y., Chen, V., 2016. Biocatalytic degradation of carbamazepine with
504   immobilized laccase-mediator membrane hybrid reactor. J. Membr. Sci. 502, 11–20.
505   https://doi.org/10.1016/j.memsci.2015.12.043

506   Ji, C., Nguyen, L.N., Hou, J., Hai, F.I., Chen, V., 2017. Direct immobilization of laccase on titania
507   nanoparticles from crude enzyme extracts of P. ostreatus culture for micro-pollutant degradation. Sep.
508   Purif. Technol. 178, 215–223. https://doi.org/10.1016/j.seppur.2017.01.043

509   Jing, X., Zhang, X., Bao, J., 2009. Inhibition Performance of Lignocellulose Degradation Products on
510   Industrial Cellulase Enzymes During Cellulose Hydrolysis. Appl. Biochem. Biotechnol. 159, 696.
511   https://doi.org/10.1007/s12010-009-8525-z

512   Jungreuthmayer, C., Steppert, P., Sekot, G., Zankel, A., Reingruber, H., Zanghellini, J., Jungbauer, A.,
513   2015. The 3D pore structure and fluid dynamics simulation of macroporous monoliths: High
514   permeability due to alternating channel width. J. Chromatogr. A 1425, 141–149.
515   https://doi.org/10.1016/j.chroma.2015.11.026

516   Kanakaraju, D., Glass, B.D., Oelgemöller, M., 2018. Advanced oxidation process-mediated removal of
517   pharmaceuticals from water: A review. J. Environ. Manage. 219, 189–207.
518   https://doi.org/10.1016/j.jenvman.2018.04.103

519   Kerrigan, J.F., Sandberg, K.D., Engstrom, D.R., LaPara, T.M., Arnold, W.A., 2018. Sedimentary record of
520   antibiotic accumulation in Minnesota Lakes. Sci. Total Environ. 621, 970–979.
521   https://doi.org/10.1016/j.scitotenv.2017.10.130

522   Kıdak, R., Doğan, Ş., 2018. Medium-high frequency ultrasound and ozone based advanced oxidation
523   for amoxicillin removal in water. Ultrason. Sonochem., SI: ESS-15, 2016, Istanbul 40, 131–139.
524   https://doi.org/10.1016/j.ultsonch.2017.01.033

525   Llorca, M., Rodríguez-Mozaz, S., Couillerot, O., Panigoni, K., de Gunzburg, J., Bayer, S., Czaja, R.,
526   Barceló, D., 2015. Identification of new transformation products during enzymatic treatment of
527   tetracycline and erythromycin antibiotics at laboratory scale by an on-line turbulent flow liquid-
528   chromatography coupled to a high resolution mass spectrometer LTQ-Orbitrap. Chemosphere 119,
529   90–98. https://doi.org/10.1016/j.chemosphere.2014.05.072

530   Lloret, L., Eibes, G., Feijoo, G., Moreira, M.T., Lema, J.M., 2012. Continuous operation of a fluidized bed
531   reactor for the removal of estrogens by immobilized laccase on Eupergit supports. J. Biotechnol.,
532   Current research and future perspectives of Applied Biotechnology 162, 404–406.
533   https://doi.org/10.1016/j.jbiotec.2012.04.007

534   Meyers, J.J., Liapis, A.I., 1999. Network modeling of the convective flow and diffusion of molecules
535   adsorbing in monoliths and in porous particles packed in a chromatographic column. J. Chromatogr. A
536   852, 3–23. https://doi.org/10.1016/s0021-9673(99)00443-4

537   Nguyen, L.N., Hai, F.I., Dosseto, A., Richardson, C., Price, W.E., Nghiem, L.D., 2016. Continuous
538   adsorption and biotransformation of micropollutants by granular activated carbon-bound laccase in a
539   packed-bed enzyme reactor. Bioresour. Technol., Special Issue on Challenges in Environmental Science
540   and Engineering (CESE-2015) 210, 108–116. https://doi.org/10.1016/j.biortech.2016.01.014

541 Nyanhongo, G.S., Nugroho Prasetyo, E., Herrero Acero, E., Guebitz, G.M., 2012. Engineering Strategies
542 for Successful Development of Functional Polymers Using Oxidative Enzymes. Chemical Engineering &
543 Technology 35, 1359-1372.

544 Ortner, A., Huber, D., Haske-Cornelius, O., Weber, H.K., Hofer, K., Bauer, W., Nyanhongo, G.S., Guebitz,
545 G.M., 2015. Laccase mediated oxidation of industrial lignins: Is oxygen limiting? Process Biochemistry
546 50, 1277-1283.

547 Parra Guardado, A.L., Belleville, M.-P., Rostro Alanis, M. de J., Parra Saldivar, R., Sanchez-Marcano, J.,
548 2019. Effect of redox mediators in pharmaceuticals degradation by laccase: A comparative study.
549 Process Biochem. 78, 123–131. https://doi.org/10.1016/j.procbio.2018.12.032

550 Patel, S.K.S., Kalia, V.C., Choi, J.H., Haw, J.R., Kim, I.W., Lee, J.K., 2014. Immobilization of Laccase on
551 SiO2 Nanocarriers Omproves Its Stability and Reusability. J. Microbiol. Biotechnol. 24, 639–647.
552 https://doi.org/10.4014/jmb.1401.01025

553 Piao, M., Zou, D., Ren, X., Gao, S., Qin, C., Piao, Y., 2019. High efficiency biotransformation of bisphenol
554 A in a fluidized bed reactor using stabilized laccase in porous silica. Enzyme Microb. Technol. 126, 1–8.
555 https://doi.org/10.1016/j.enzmictec.2019.03.006

556 Rajapaksha, A.U., Dilrukshi Premarathna, K.S., Gunarathne, V., Ahmed, A., Vithanage, M., 2019. 9 -
557 Sorptive removal of pharmaceutical and personal care products from water and wastewater, in:
558 Prasad, M.N.V., Vithanage, M., Kapley, A. (Eds.), Pharmaceuticals and Personal Care Products: Waste
559 Management and Treatment Technology. Butterworth-Heinemann, pp. 213–238.
560 https://doi.org/10.1016/B978-0-12-816189-0.00009-3

561 Rocha, L.S., Pereira, D., Sousa, É., Otero, M., Esteves, V.I., Calisto, V., 2020. Recent advances on the
562 development and application of magnetic activated carbon and char for the removal of
563 pharmaceutical compounds from waters: A review. Sci. Total Environ. 718, 137272.
564 https://doi.org/10.1016/j.scitotenv.2020.137272

565 Sadeghzadeh, S., Ghobadi Nejad, Z., Ghasemi, S., Khafaji, M., Borghei, S.M., 2020. Removal of
566 bisphenol A in aqueous solution using magnetic cross-linked laccase aggregates from Trametes
567 hirsuta. Bioresour. Technol. 306, 123169. https://doi.org/10.1016/j.biortech.2020.123169

568 Sebai, W., Ahmad, S., Belleville, M.-P., Boccheciampe, A., Chaurand, P., Levard, C., Brun, N., Galarneau,
569 A., Sanchez-Marcano, J., 2022. Biocatalytic Elimination of Pharmaceutics Found in Water With
570 Hierarchical Silica Monoliths in Continuous Flow. Front. Chem. Eng. 4.

571 Sheldon, R.A., 2007. Enzyme immobilization: The quest for optimum performance. Adv. Synth. Catal.
572 349, 1289–1307. https://doi.org/10.1002/adsc.200700082

573 Singh Arora, D., Kumar Sharma, R., 2010. Ligninolytic Fungal Laccases and Their Biotechnological
574 Applications. Appl. Biochem. Biotechnol. 160, 1760–1788. https://doi.org/10.1007/s12010-009-8676-y

575 Tallarek, U., Leinweber, F.C., Seidel-Morgenstern, A., 2002. Fluid Dynamics in Monolithic Adsorbents:
576 Phenomenological Approach to Equivalent Particle Dimensions. Chem. Eng. Technol. 25, 1177–1181.
577 https://doi.org/10.1002/1521-4125(20021210)25:12<1177::AID-CEAT1177>3.0.CO;2-V

578 Thiebault, T., Boussafir, M., Le Milbeau, C., 2017. Occurrence and removal efficiency of
579 pharmaceuticals in an urban wastewater treatment plant: Mass balance, fate and consumption
580 assessment. J. Environ. Chem. Eng. 5, 2894–2902. https://doi.org/10.1016/j.jece.2017.05.039

581   Verlicchi, P., Al Aukidy, M., Zambello, E., 2012. Occurrence of pharmaceutical compounds in urban
582   wastewater: Removal, mass load and environmental risk after a secondary treatment—A review. Sci.
583   Total Environ., Special Section - Arsenic in Latin America, An Unrevealed Continent: Occurence, Health
584   Effects and Mitigation 429, 123–155. https://doi.org/10.1016/j.scitotenv.2012.04.028

585   Zdarta, J., Feliczak-Guzik, A., Siwińska-Ciesielczyk, K., Nowak, I., Jesionowski, T., 2020. Mesostructured
586   cellular foam silica materials for laccase immobilization and tetracycline removal: A comprehensive
587   study. Microporous Mesoporous Mater. 291, 109688.
588   https://doi.org/10.1016/j.micromeso.2019.109688

589   Zdarta, J., Meyer, A.S., Jesionowski, T., Pinelo, M., 2018. Developments in support materials for
590   immobilization of oxidoreductases: A comprehensive review. Adv. Colloid Interface Sci. 258, 1–20.
591   https://doi.org/10.1016/j.cis.2018.07.004

592   Zhang, Y., Ge, J., Liu, Z., 2015. Enhanced Activity of Immobilized or Chemically Modified Enzymes. ACS
593   Catal. 5, 4503–4513. https://doi.org/10.1021/acscatal.5b00996

594   Zheng, F., Cui, B.K., Wu, X.J., Meng, G., Liu, H.X., Si, J., 2016. Immobilization of laccase onto chitosan
595   beads to enhance its capability to degrade synthetic dyes. Int. Biodeterior. Biodegrad. 110, 69–78.
596   https://doi.org/10.1016/j.ibiod.2016.03.004

597

598

599